SCIENCE CHINA
Earth Sciences

•RESEARCH PAPER•

May 2018 Vol.61 No.5: 614–624
https://doi.org/10.1007/s11430-017-9186-9

Progress and performance evaluation of BeiDou global navigation satellite system: Data analysis based on BDS-3 demonstration system

Yuanxi YANG[1*], Yangyin XU[2†], Jinlong LI[3] & Cheng YANG[4]

[1] *State Key Laboratory of Geo-information Engineering, Xi'an 710054, China;*
[2] *Institute of Geographical Spatial Information, Information Engineering University, Zhengzhou 450001, China;*
[3] *Beijing Satellite Navigation Center, Beijing 100094, China;*
[4] *School of Land Science and Geomatics, China University of Geosciences, Beijing 100083, China*

Received December 11, 2017; revised February 23, 2018; accepted March 8, 2018; published online March 29, 2018

Abstract The first two Medium Earth Orbit (MEO) satellites of the third generation of BeiDou satellite navigation System (BDS-3) were successfully launched on November 5, 2017. This historical launch starts the new era of the global navigation satellite system of BeiDou. Before the first two satellites of BDS-3, a demonstration system for BDS-3 with five satellites, including two Inclined Geosynchronous Orbit satellites (IGSO) and three MEO satellites, was established between 2015 and 2016 for testing the new payloads, new designed signals and new techniques. In the demonstration system, the new S frequency signal and satellite hydrogen clock as well as inter-satellite link (ISL) based on Ka-band signals with time-division multiple addresses (TDMA) were tested. This paper mainly analyzes the performances of the demonstration system, including the signal-to-noise ratios, pseudorange errors and the multipath errors of the civilian signals of BDS-3. The qualities of signals in space, time synchronization and timing precision were tested as well. Most of the performances were compared with those of the regional BeiDou satellite navigation system (BDS-2). At last, the performances of positioning, navigation and timing (PNT) of the future BeiDou global system (BDS-3) were evaluated based on the signal quality of the present demonstration satellite system.

Keywords BeiDou-3, Demonstration satellite, Signal, Timing, Signal-to-noise ratios

Citation: Yang Y, Xu Y, Li J, Yang C. 2018. Progress and performance evaluation of BeiDou global navigation satellite system: Data analysis based on BDS-3 demonstration system. Science China Earth Sciences, 61: 614–624, https://doi.org/10.1007/s11430-017-9186-9

1. Introduction

According to the three-step development strategy, BeiDou satellite navigation system has completed the BeiDou demonstration system (1990−2003), simply called BDS-1, and the regional BeiDou satellite navigation system (2003−2012), referred to as BDS-2. And now the BeiDou global satellite navigation system is under construction, which is a global service system and called BDS-3.

The BDS-1 started its service from 2003, including positioning, timing and short message communication (Yang, 2010; Yang et al., 2011). BDS-1 provides services based on two geosynchronous orbit (GEO) satellites with additional backup satellite, using transparency retransmission mode. As the three dimensional (3-D) coordinates cannot be obtained directly by just measuring the ranges from the receiver to only two satellites, the measured ranges are first transmitted to the ground control center, where the 3-D coordinates can be calculated by mapping the ranges with the topographic map, and then the control center transmits the coordinates

* Corresponding author (email: yuanxi_yang@163.com)
† Corresponding author (email: xu_yangyin@163.com)

back to the users by an encrypted satellite link. Apparently, this method needs to build a data channel between the users and the control center to achieve a two-way communication, which provides a basis for achieving the location tracking service and the short message communication service (Tan, 2010; Gu et al., 2015). The positioning accuracy provided by BDS-1 can reach 20 m; the time accuracy is able to achieve 100 ns with one-way timing method, and 20 ns with round-way timing method. The short message communication service has the capacity to transmit a message within 240 bites. The BDS-1, however, cannot provide dynamic positioning services.

The BDS-2 became operational in 2012 (Yang et al., 2014). It consists of 5 GEO satellites, 5 Inclined Geosynchronous Orbit (IGSO) satellites and 4 Medium Earth Orbit (MEO) satellites. And its service covers the area from 55°S to 55°N latitude and 55°E to 180°E longitude, which covers 94.6% of Asia-Pacific area. The system not only continues the service of positioning, timing and short message communication like BDS-1 does, but also provides kinematic positioning. Furthermore, the BDS-2 significantly improves the positioning and timing accuracy. The whole constellation of BDS-2 broadcasts triple frequency signals B1, B2 and B3. Compared with dual-frequency signals, Triple frequency signals can provide more combinations with excellent characteristics (Li J L et al., 2012, 2017), speed up the carrier phase ambiguity resolution (Feng, 2008; Geng and Bock, 2014; Li J L et al., 2013), be beneficial for long distance RTK solution (Li B F et al., 2017) and improve the accuracy and reliability of positioning (Li B F et al., 2013).

Since the BDS-2 provided its service, most of the performance indexes have been sufficiently verified, including the accuracy of signal in space, performances of the satellite orbit determination and satellite clock, the accuracy of positioning and timing etc. The precision of BDS-2 B1 code and carrier phase measurement are about 11 cm and 0.5 mm respectively, and that of B2 code and carrier phase measurement are about 5 cm and 0.3 mm. And the single point positioning by using B1 code measurements can achieve 6 m in the horizontal component and 10 m in the vertical component (Yang et al., 2014). The research towards the orbit determination of BDS-2 has been reported (He et al., 2013; Shi et al., 2012). In general, the radial accuracy of the broadcast orbits is better than 0.5 m for IGSO and MEO satellites, and 1.0 m for GEO satellites; and the orbit accuracy of the precise ephemeris is better than 10.0 cm in the radial direction for IGSO and GEO satellites, and about 50.0 cm for GEO satellites (Peng et al., 2016; Shi et al., 2012). During the satellite eclipse period, especially in the yaw-maneuver period, the orbit accuracies of IGSO and MEO satellites are degraded; the orbit error of the broadcast ephemeris is about 1.5–2.0 m in the radial component, but that of the precise ephemeris can exceed 10.0 cm in the radial component (Peng et al., 2016). The differences between the satellite precise clock offset products provided by the BeiDou analysis centers are usually about 0.5 to 0.8 ns for GEO satellites, 0.2 to 0.3 ns for IGSO satellites and 0.15 to 0.2 for MEO satellites (Guo et al., 2016). The frequency stability of the rubidian clock onboard of the BDS-2 satellites is about 7×10^{-12}–1×10^{-11} at 1 second, 1×10^{-13} at one thousand seconds and 2.53×10^{-14}–9.38×10^{-14} at one day (Han et al., 2013). The timing accuracy can achieve 50 ns in one-way timing service and 10 ns in two-way timing service (Han et al., 2011). Also, the position accuracies for different positioning modes of BDS-2 have also been researched (Shi et al., 2013; He et al., 2014; Li J L et al., 2017).

The global BDS (BDS-3) was started in 2016. It consists of 3 GEO satellites, which will be located at 80°E, 110.5°E and 140°E, respectively; 3 IGSO satellites with 55° orbit inclinations, and 24 MEO satellites located in three orbit planes with 21528 km altitude and 55° orbital inclinations. And the constellation will be fully operational by 2020 (China Satellite Navigation Office, 2017a).

On November 5, 2017, the first two BDS-3 satellites were launched (SV number 19 and 20), which means that the China BDS starts its global system construction. But before the launch of the first two BDS-3 satellites, a demonstration system with five satellites, including two IGSO satellites, I1-S and I2-S, and three MEO satellites, M1-S, M2-S, and M3-S, had been established since 2015 to fully verify the design of the BDS-3. The demonstration system transmits signals on four frequencies at 1575.420 MHz (B1), 1191.795MHz (B2), 1268.520MHz (B3) and 2492.028 MHz (Bs). The inter-satellite link was built on the demonstration system based on the Ka-band signals and the new hydrogen clock was employed on one satellite. Based on the demonstration system, the synergy and coordination status among the satellites and the control center, the inter-satellite links, and the uploading injection and downloading reception signal have been tested under different conditions; and the quality of the receiving signals has also been monitored and analyzed. At the same time, the performance of the BDS-3 precision orbit determination, positioning, velocity and timing (PVT) indexes have also been validated and evaluated. Thus, the PNT performance of the future BDS-3 has been comprehensively tested and evaluated.

This paper is mainly designed to make a relatively comprehensive evaluation of the performance of the BeiDou global navigation satellite system based on the data analysis of the BDS-3 demonstration system. In the second part, the frequency design and satellites basic payloads of BDS-3 are introduced. The third part mainly focuses on the analysis of the BDS-3 user application performances, including the signal-to-noise ratio of each frequency signal, the precision of the single frequency pseudorange measurement and user timing accuracy, etc. At last, the possible performances of the

global BDS-3 are predicted based on the tested signal qualities and the designed BDS-3 constellation.

2. The basic performance of the demonstration system

The BDS-3 not only has a significant improvement over the BDS-2 in terms of satellite constellation, but also has made great adjustments in many other aspects. In terms of satellite payloads, new hydrogen atomic clock, inter-satellite links based on the Ka-band signal, and the satellite antenna for broadcasting S-band signals have been added to the BDS-3 test satellite; in the aspect of signal design, BDS-3 also has great improvement compared with BDS-2, see Table 1. The new designed signals of BDS-3 partly overlap with GPS, Galileo, QZSS and INSS, which is beneficial for improving the compatibility and interoperability among the different systems. As the L band radio frequencies are crowed in satellite navigation, the new designed S-band signal, Bs, on BDS-3 will increase the frequency source for the future satellite navigation system (Tan, 2017). In addition, in order to realize the smooth transition from BDS-2 to BDS-3, the demonstration satellite system not only transmits the new designed signals but also transmits the B1I and B3I/Q signals of BDS-2. The satellite I1-S only transmits B1I and B3I/Q signals of BDS-2, while the satellites I2-S, M1-S and M2-S transmit the new designed signals of BDS-3 and B1I and B3I/Q signals. The signal Bs is only transmitted by I2-S and M1-S satellites. The M3-S is only used for on-orbit testing and has not been officially put into use.

The frequency stability of the atomic clock on the demonstration system is about 10^{-14} at one day for the rubidium atomic clock and about 10^{-15} at one day for the hydrogen clock, which is improved compared to the atomic clocks on the BDS-2. The accuracy of time synchronization between the satellites-ground, satellite-satellite, and station-station is about 0.14 ns. The two hour prediction accuracy of satellite clock error is about 0.4 ns, which is significantly improved compared with BDS-2 (China Satellite Navigation Office, 2017b).

The orbit accuracy of the multi-satellites overall orbit determination is better than 1.5 m. The user range prediction accuracy in 2 hours is about 0.5 m. The joined orbit determination with satellite-ground and satellite-satellite observations is about 1 m, and the prediction accuracy in 2 hours is about 0.31 m, which is better than those determined only by satellite-ground observations (Chen et al., 2016; Tang et al., 2017). The accuracy along track (T component) of the orbit is greatly improved by 63.1%, and the accuracy of the orbit prediction is improved by 75.7%, due to the constraints in the T and normal component (N) by ISL. The joint prediction of clock offset improves from 0.4 ns to 0.3 ns for IGSO satellites and from 1.1 to 0.5 ns for MEO satellites. The improvement reaches 53.9% compared to those determined only using satellite-ground link observations. The autonomous orbit determination accuracy can achieve 6 m by using the inter-satellite link with support of the prior meter-level orbit determined by the control center using L band (Ren et al., 2017).

The range accuracy for the monitoring receiver is about 0.04 ns and for the multi-frequency receiver is 0.1–0.4 m. The velocity accuracy is 0.03 m/s (95%). As we know that the demonstration system of BDS-3 cannot provide positioning service in most cases due to not enough satellites. By combining BDS-2 and the demonstration satellites of BDS-3, we can get 3.5 to 4.3 m single frequency positioning accuracy in the horizontal components and 3.8 to 5.9 m in the vertical component (China Satellite Navigation Office, 2017b).

3. Performance analysis of user's monitoring

To verify the potential performance of the future global BDS, the performance in the users' side are analyzed, the emphasis of which is on the prediction of the performance based on the analyzed demonstration signal quality and the constellation geometry of the BDS-3.

3.1 Analysis of signal-to-noise ratio

The satellite Signal-to-Noise Ratio (SNR) is an index of the signal quality and related to the accuracy of the carrier phase measurement (Zhang and Ding, 2013). The variations of the SNR with elevation angle of the test satellite signals are firstly analyzed in this paper. The experimental test is conducted in Zhengzhou area, China. The data are collected between 20th and 26th Oct. 2017 using the receiver produced by Chengdu Guoxing Company. The sampling rate is 30 s, and the cutoff elevation angle is set to 10°. With the SNR being averaged by every 2° elevation angle, Figure 1 shows the SNR versus satellite elevation angle of the B1C, B1I, B2b, B2a+b, B3I and Bs signals on I2-S and M1-S satellites. (The SNR of B2a signal is not involved, due to the receiver problems).

From Figure 1, we find that different signals have nearly the same tendency of the SNR versus satellite elevation angle, which can be interpreted that the SNR increases as the elevation angle increases. It is also noted that the SNR of MEO satellites is about 2–3 dB larger than that of IGSO at the same elevation angle, the reason of which may be that the IGSO satellites have higher altitude and less transmission power than those of MEO satellites.

The SNR versus satellite elevation angle of Bs signal, which is plotted by red-dot line, exhibits abnormal behavior,

Table 1 Comparison of frequency distribution between BDS-3 and other satellite navigation system

Band	Frequency (MHz)	GPS	Galileo	BDS-2	QZSS	IRNSS	BDS-3 Test System
S	2492.028					Bs	Bs
L	1575.420	L1	E1		L1		B1
	1561.098			B1			
	1278.750		E6				
	1268.520			B3			B3
	1227.600	L2			L2		
	1207.140		E5b	B2			B2b
	1191.795		E5				B2a+b
	1176.450	L5	E5a		L5	L5	B2a

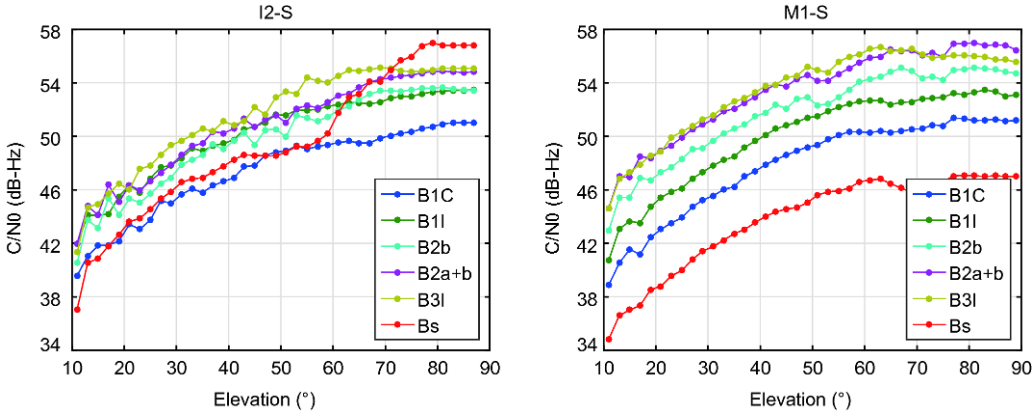

Figure 1 Measured signal-to-noise ratio versus elevation angle of BDS-3 test system satellites signals.

and it performs different between IGSO and MEO satellites. For I2-S satellites, the SNR of Bs signal changes significantly with the elevation angle. And it is smaller than those of other signals at low elevation angle, but bigger at high elevation angle, as it increases quickly as elevation angle increases. For M1-S satellite, the SNR of Bs signal is smaller than those of other signals all the time, the reason of which might be the lower transmission power of M1-S, see Figure 1.

3.2 Pseudorange noises analysis

Pseudorange noise is one of the basic performances that the users are most concerned about, because that most of the users can only afford low-cost single frequency navigation receivers. The performance of the single frequency pseudorange noises is analyzed based on the time-differenced code minus phase (CC) combination (de Bakker et al., 2009). Time-differenced CC combination can eliminate the carrier phase ambiguity and weaken the ionospheric delay, hardware delay and multipath effect. The remaining error mainly reflects the pseudorange noise. In our test, the time series of the time-differenced CC combination are calculated for each navigation signal, and then the Root Mean Square (RMS) errors relative to zero mean are obtained in every 10° elevation angle interval. At last, the calculated RMS is transformed into the RMS of un-differenced pseudorange noise for each navigation signal. Figure 2 shows the variations of the un-differenced pseudorange noise with satellite elevation angle of different signals on satellites I2-S and M1-S. It is obvious that all the frequency signal noises for both IGSO and MEO satellites change with the elevation angles. And the similar phenomenon is shown in the other two satellites I1-S and M2-S, which is omitted in this paper.

From Figure 2, we find that:

(1) The pseudorange noises of each frequency signal decreases as the elevation angle increases, and tends to be stable when the elevation angle is greater than 50°.

(2) The RMS of B1C signal is higher than those of other signals at the same elevation angle. The RMS of the pseudorange noises of B2a+b is the smallest.

(3) By comparing the pseudorange noise within the same type of satellite, IGSO and MEO, it can be noticed that the pseudorange measurement accuracy of the same signal is similar among the same type of satellites.

(4) It should be noted that the RMS of the pseudorange noise of MEO satellites is larger than that of IGSO satellites, and the reason may be that the ratio of low-elevation ob-

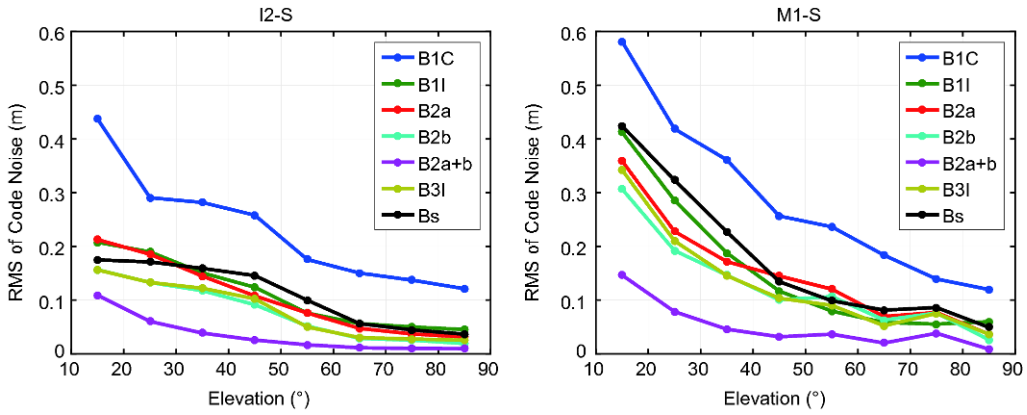

Figure 2 RMS of code noise versus elevation angle of BDS-3 test system satellites signals.

servations of MEO satellites in the observation arc is more than that of IGSO satellites.

(5) It can also be found that B1C signal has the worst pseudorange measurement accuracy among the signals while B2a+b signal has the best; the pseudorange measurement accuracy of Bs signal is worse than that of B2a+b, but better than that of the B1C signal.

3.3 Pseudorange multipath analysis

The multipath error affects the satellite orbit determination and user's positioning accuracy. Previous study has pointed out that there are systematic errors related to elevation angle exist in the pseudorange multipath of BDS-2 triple frequencies signals (Wanninger and Beer, 2015). This kind of systematic errors may be caused by the satellite-induced multipath error and can influence the performance of positioning. We use multipath combination (MP) to analyze the multipath of the test satellites of BDS-3 (de Bakker et al., 2009; Wanninger and Beer, 2015). Figure 3 presents the time series of the multipath combination of BDS-3 signals of I2-S and M1-S satellites, and Figure 4 shows the RMS of the multipath of different signals on I1-S, I2-S, M1-S and M2-S satellites.

From the Figure 3 and 4, we find that:

(1) The pseudorange multipath effect of the BDS-3 global system signal is obviously reduced, and there is almost no obvious systematic error that related to the elevation angle.

(2) Among the different signals, B2a+b signal has the strongest anti-multipath ability, while the B1C has the worst.

(3) Unlike other signals, the multipath of Bs signal has some systematic trends on IGSO and MEO satellites, as shown in Figure 3. This may be caused by the difference between the S frequency and L frequency antenna.

(4) The RMS of MEO multipath errors is larger than that of IGSO satellite. In our opinion, this phenomenon is partly caused by the large proportion of low-elevation observations of MEO satellites during the observation period.

To compare the multipath effects of BDS-3 and BDS-2, we calculated the multipath on B1I and B3I frequencies of MEO and IGSO satellites. The time series of the multipath of MEO satellites are presented in Figure 5 and that of the IGSO satellites are plotted in Figure 6; Figure 7 illustrates the RMS of the multipath errors on B1I and B3I signal of all IGSO and MEO satellites of BDS-2 and the BDS-3 demonstration system.

From Figure 5, 6 and 7, we can conclude that:

(1) The pseudorange multipath effect of B1I and B3I signals on BDS-3 test satellites is less than that of BDS-2 satellites, as there are systematic errors associated with elevation angles exist in the pseudorange multipath of BDS-2 satellite. However, no obvious such systematic errors have been observed in the pseudorange multipath of BDS-3 test satellites.

(2) In Figure 7, we find that the IGSO satellites, which are C06-C10 of BDS-2 and I1-S, I2-S of BDS-3, have less pseudorange multipath errors than those of MEO satellites.

(3) The pseudorange multipath of B3I signal is less than that of B1I signal. Therefore, the BeiDou ICD suggested using B3I signal as the reference of frequency bias.

3.4 Signal-in-space quality and timing accuracy

The User Equivalent Range Error (UERE) is often used to represent the signal-in-space quality, and its quantity reflects the single point positioning accuracy (Montenbruck et al., 2015). The UERE could be calculated via,

$$\begin{aligned}&\mathrm{UERE}^{s}_{r,j}\\&= p^{s}_{r,j} - \left(\overline{\rho}^{s}_{r} - \overline{dt}^{s}_{,\mathrm{eph}} + \overline{\mathrm{TGD}}^{s}_{,j} + \bar{\imath}^{s}_{r,j} + \bar{v}^{s}_{r}\right)\\&= dt_{r,j} + \Delta\rho^{s}_{r} - \Delta dt^{s}_{,\mathrm{eph}} + \Delta\mathrm{TGD}^{s}_{,j}\\&+\Delta\imath^{s}_{r,j} + \Delta v^{s}_{r} + e^{s}_{r,j},\end{aligned} \tag{1}$$

where $p^{s}_{r,j}$ is the pseudorange measurement between receiver r and satellite s at the navigation signal j; ρ^{s}_{r} is the distance between the satellite and receiver; $dt_{r,j}$ is the receiver clock

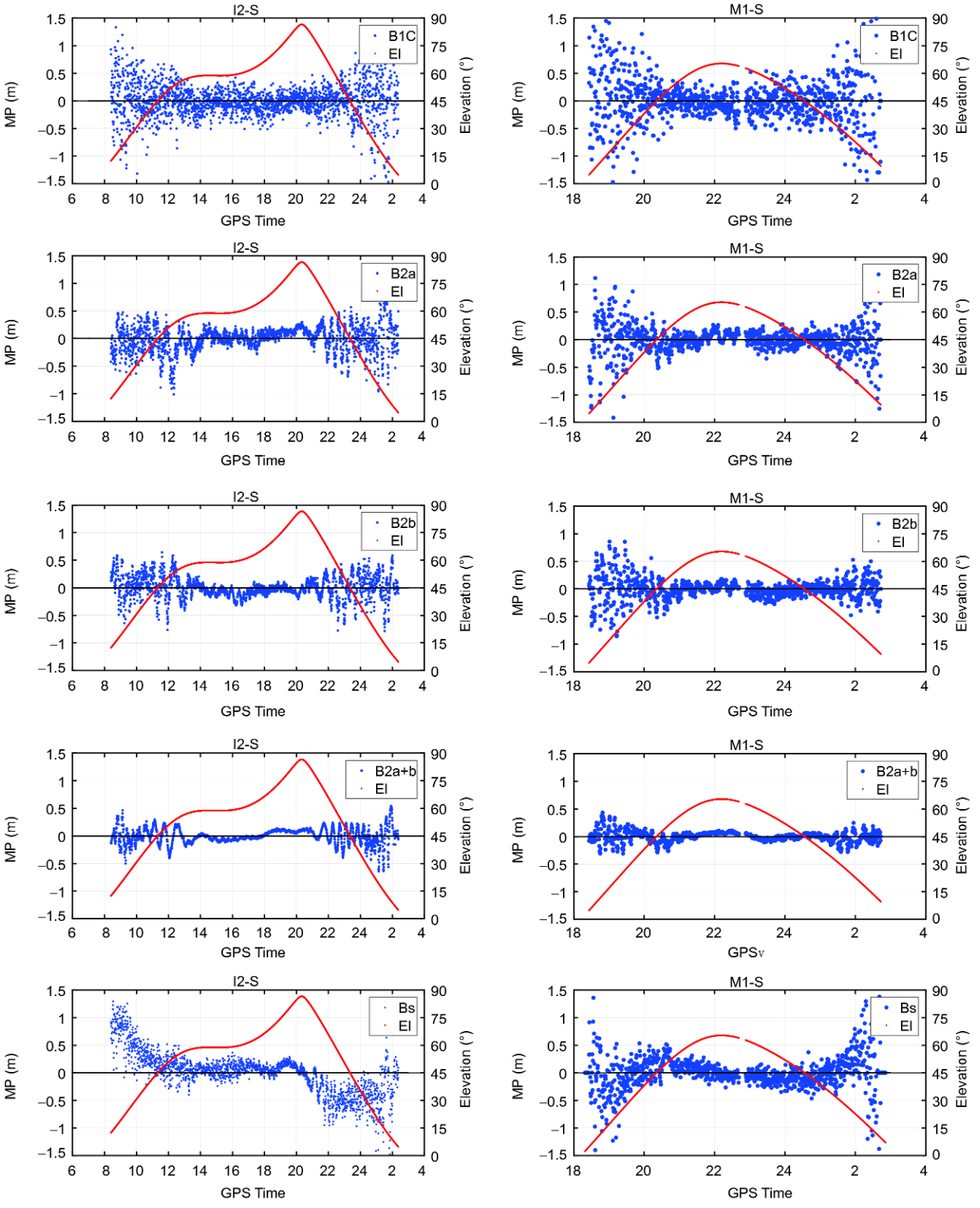

Figure 3 MP time series of BDS-3 new designed signals of I2-S and M1-S satellites.

bias; $dt^s_{,\mathrm{eph}}$ is the satellite clock bias; $\mathrm{TGD}^s_{,j}$ is the satellite equipment delay; $\iota^s_{r,j}$ and v^s_r are the ionosphere and tropospheric delay, respectively; $e^s_{r,j}$ is the unmolded error. $\overline{\rho}^s_r$, $\overline{dt}^s_{,\mathrm{eph}}$, $\overline{\mathrm{TGD}}^s_{,j}$, $\bar{\iota}^s_{r,j}$ and $\bar{v}^s_r$ are the model corrections calculated

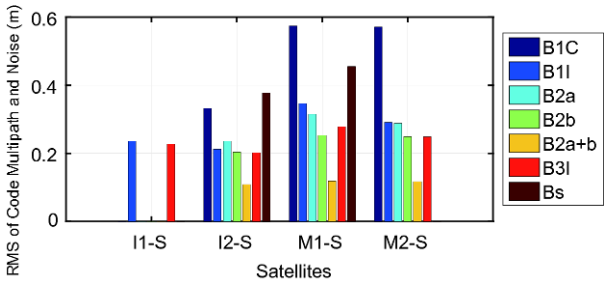

Figure 4 RMS of code multipath of testing satellites.

according to the navigation message. Δ denotes the residual error after the compensation of the model correction.

In order to assess the signal-in-space quality of the test satellites, we used a BDS-3 test terminal to monitor B1I and B3I signals of the four test satellites in Beijing from March 3 to March 9, 2017. In the experiment, UERE of B1I and B3I signals of each test satellite are calculated according to Formula (1), and the daily average value of the corresponding UERE is derived. The statistical results are shown in Table 2.

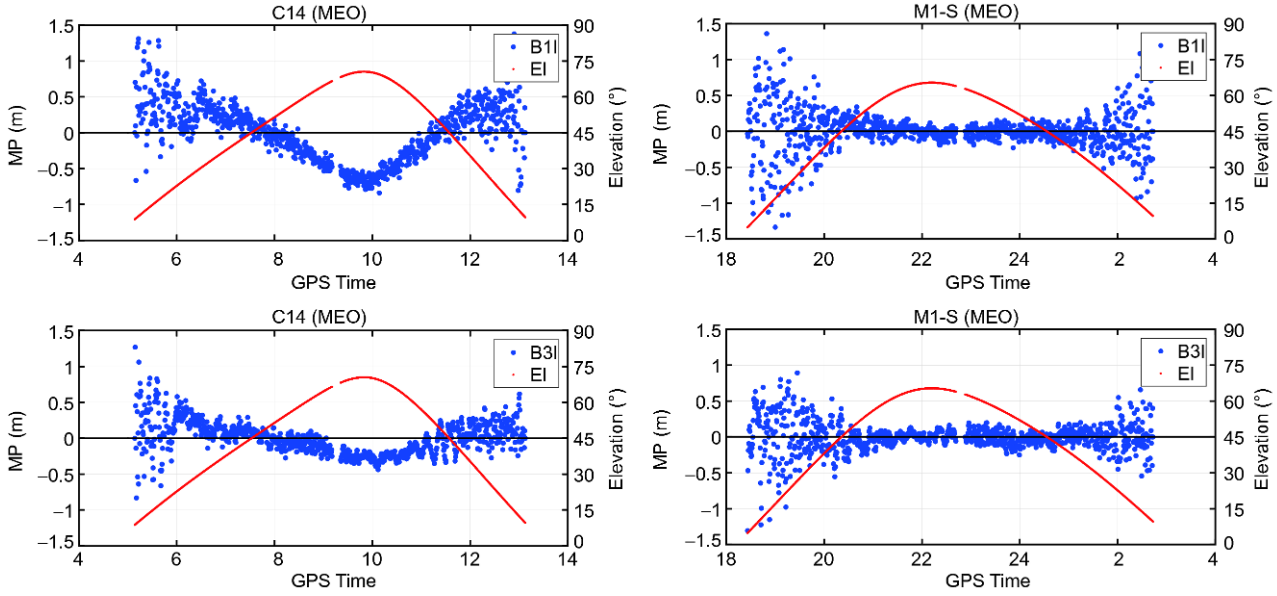

Figure 5 MP time series of B1I and B3I signals of the MEO satellite of BDS-2 and the BDS-3 demonstration system. C14 represnts the MEO satellite of BDS-2, and M1-S represnts that of BDS-3.

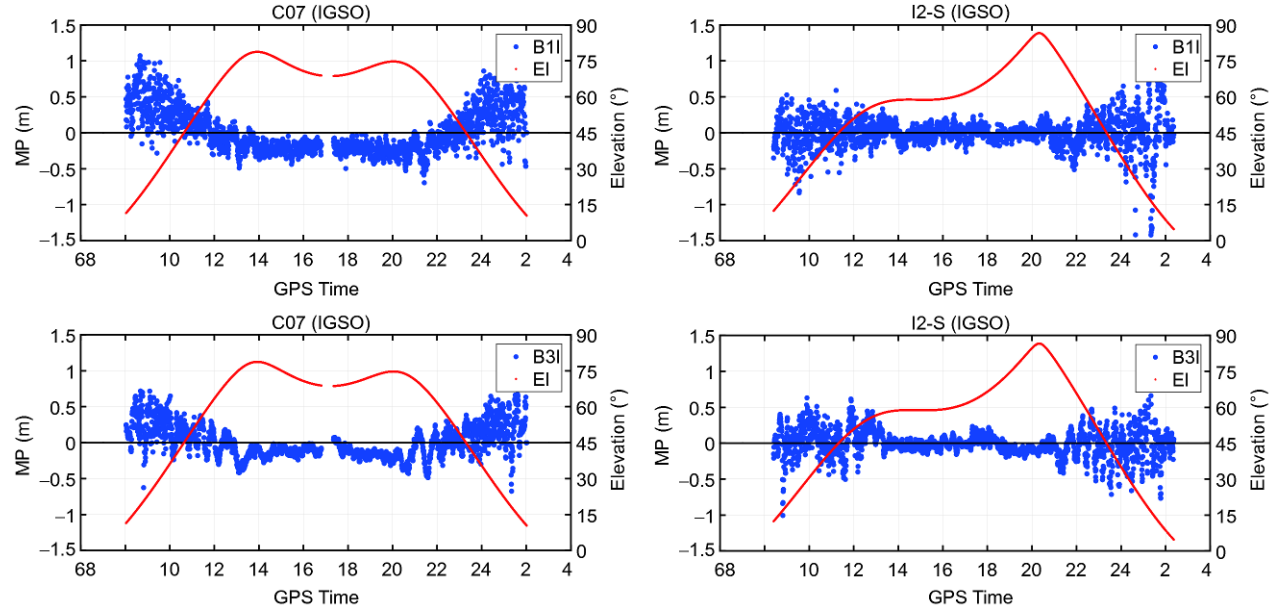

Figure 6 MP time series of B1I and B3I signals of the IGSO satellite of BDS-2 and the BDS-3 demonstration system. C07 represnts the IGSO satellite of BDS-2, and I2-S represnts that of BDS-3.

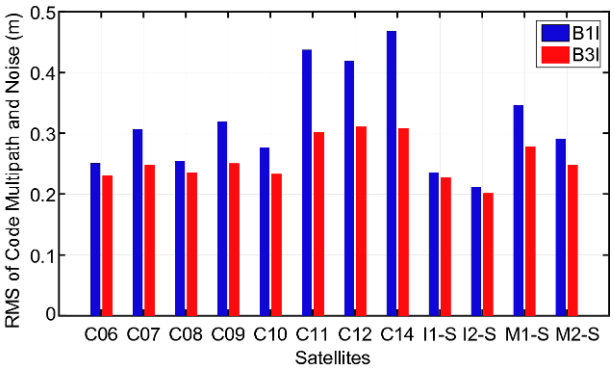

Figure 7 RMS of code multipath of B1I and B3I signals. C*i* represnt satellites of BDS-2, and I or M represnt that of BDS-3.

From the Table 2, we can find that the UERE of IGSO satellites of BDS-3 is better than that of MEO satellites. The reason may be that the MEO satellite has less observable time and the observation ratio of the mid- and low-elevation angle in the satellite observation period is relatively large.

In addition, Table 3 presents the timing accuracies of BDS-3 test satellites monitored by Beidou satellite operation and control system using multi-frequency receiver and compatible receiver. Among them, the timing accuracy is calculated by extracting time parameters from the user pseudorange observation equations. In the calculation, the user position is known and fixed, the satellite orbit, satellite clock offset, ionospheric and tropospheric delay parameters are calculated from the navigation ephemeris.

From the Table 3, it is easy to find that the timing accuracies are different with different receivers and different signals. Most of the timing accuracies are better than 10 ns, while the worst is about 21.95 ns.

4. The accuracy prediction of the global system of BDS

In this part, the possible positioning and navigation accuracy for the coming BDS-3 is analyzed based on the signal quality of the test constellation and the simulated BDS-3 constellation, which is consisted by 3 GEO satellites, 3 IGSO satellites, and 24 MEO satellites (China Satellite Navigation Office, 2017a). The design of the constellation is shown as follows (China Satellite Navigation Office, 2013).

(1) The orbit of GEO satellites is 35786 km high, positioned at 80°E, 110.5°E and 140° E.

(2) The orbit of IGSO satellites is 35786 km high with 120° spacing in the right ascension of ascending node and with inclination angle of 55°. The three IGSO satellites are overlapped with intersection point at longitude 118 °E.

(3) The altitude of MEO satellites is 21528 km with inclination angle of 55°. The MEO satellites orbit distribute in

Table 2 BDS-3 daily UERE of BDS-3 test satellites (Unit: m)

Days	I1-S		I2-S		M1-S		M2-S	
	B1I	B3I	B1I	B3I	B1I	B3I	B1I	B3I
03.03	–0.82	–0.60	0.19	–0.12	0.93	1.14	1.63	1.51
04.03	–0.55	–0.27	0.07	–0.17	0.26	0.33	1.21	0.98
05.03	–1.04	–0.81	0.28	0.11	0.76	1.10	1.24	1.04
06.03	–0.79	–0.51	0.09	–0.14	0.78	0.94	0.94	0.72
07.03	–0.97	–0.71	0.01	–0.32	0.89	1.10	1.57	1.45
08.03	–0.75	–0.51	0.25	–0.05	0.85	1.00	0.89	0.70
09.03	–0.85	–0.67	0.39	0.08	1.12	1.35	–0.35	–0.65
Average	–0.82	–0.58	0.18	–0.09	0.80	0.99	1.02	0.82

Table 3 Timing accuracy of BDS-3 test satellites (ns)[a)]

Item		I1S	I2S	M1S	M2S
multi-frequency receiver	B1I	7.36	8.48	7.10	9.05
	B1C	-	9.66	4.50	10.27
	B2a	-	13.68	5.00	9.49
	B2b	-	6.18	5.37	7.61
	B2a+b	-	10.25	8.10	5.73
	B3I	12.59	7.41	6.23	7.13
compatible receiver	B1I	11.89	6.53	12.78	21.95
	B1C	-	4.98	7.80	21.71
	B2a	-	4.31	8.74	11.48

a) The results of table 3 are provided by Dr. Jinxian ZHAO.

Walker 24/3/1 constellation. The first, second and third orbit planes distribute with right ascension of ascending node of 0°, 120° and 240° respectively. The angular distance of ascending node of the first satellite in these three orbit planes are 0°, 15° and 30° respectively.

The regression period of MEO satellites is 7 days and 13circles, thus, the simulation time is set to be 7 days, the-simulation sampling interval is 300 s, and the interval oflongitude and latitude is set to 5°×2.5°. When the cutoff elevation angle is set to 5°, the satellite visible geometry at global scale including the number of visible satellite (NSAT), PDOP, HDOP and VDOP is simulated and presented in Figures 8 to 11.

We find that the number of visible satellites of BDS-3 in global scale is from 6 to 13; and there are at least 6 visible satellites within the area 150° W to 10°E and 15° S to 55° N. There are more than 11 visible satellites between 70°E to 150°E and 75°N to 75°S; and more than 13 visible satellites around the area of the equatorial zone.

From the Figure 9, the PDOP value of BDS-3 is within 1.3 to 2.7 in global scale. If the UERE is 1 m, the BDS-3 is able to achieve 1.3 to 2.7 m positioning accuracy.

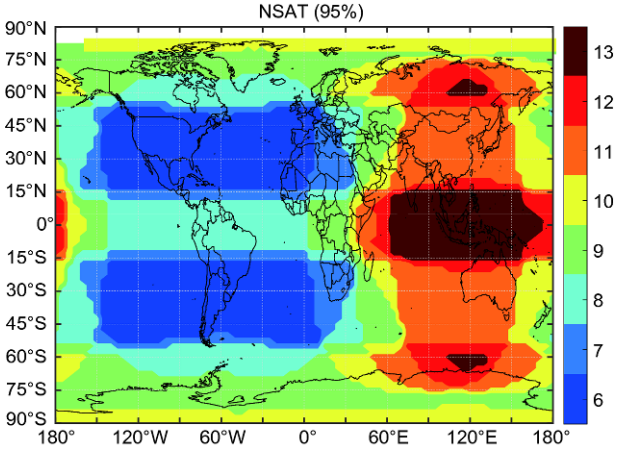

Figure 8 Distribution of visible satellites.

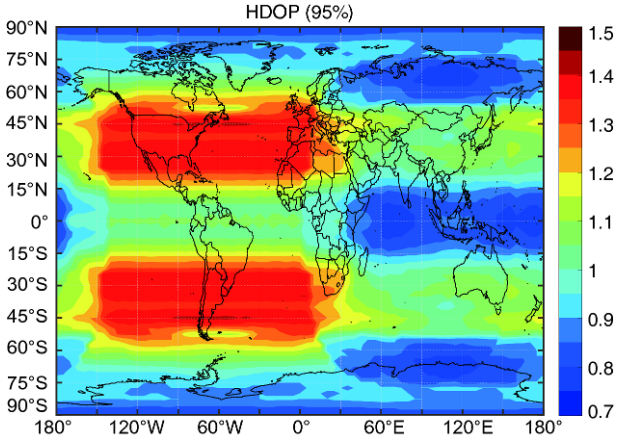

Figure 10 Distribution of HDOP.

From the Figure 10, we find that the HDOP value of BDS-3 is within 0.7 to 1.5 in global scale. Thus, the horizontal positioning accuracy provided by future BDS-3 will arrive at 0.7 to 1.5 m if UERE is 1 m.

From the Figure 10, we also find that the VDOP value of BDS-3 is within 1.1–2.4 in global scale. Thus, the vertical positioning accuracy is able to achieve 1.1–2.4 m for BDS-3 if UERE is 1 m.

However, the UERE acquire in China territory could not represent the global signal quality of BDS-3, because the tracking stations for the determination of satellite orbit and satellite clock offset are located in China at present.

5. Conclusions

This paper introduced the frequencies design of BDS-3 and the payloads of the test satellites. Focused on the performance of BDS-3 from the perspective of the users, The SNR of the signals, multipath errors of pseudorange measurements and the signal-in-space quality, as well as the positioning and timing accuracy are analyzed. Finally, based on

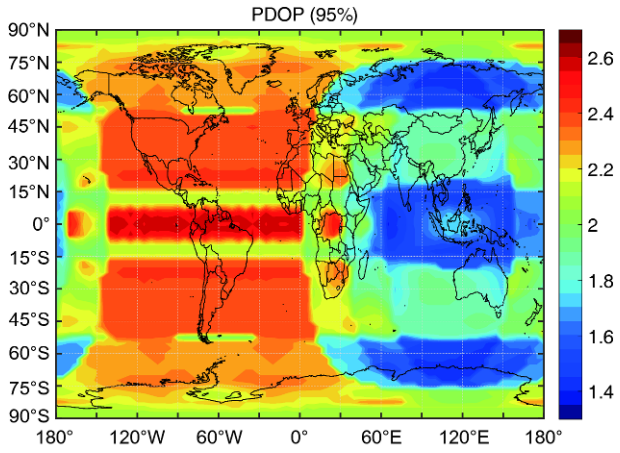

Figure 9 Distribution of PDOP.

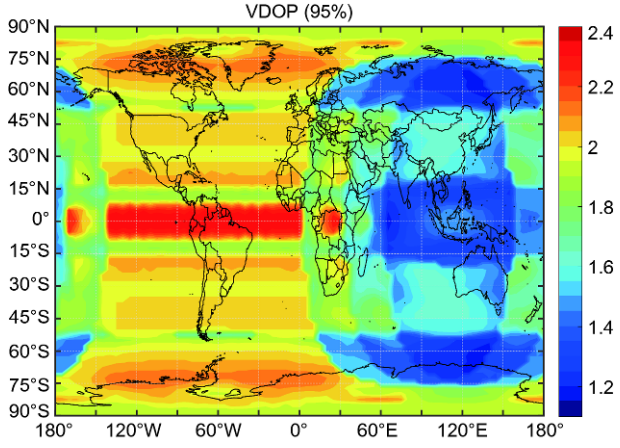

Figure 11 Distribution of VDOP.

the tested signal qualities and the designed BDS-3 constellation, a simple prediction of the possible performance of the BDS-3 full constellation is carried out. The results can be summarized as below:

(1) Among the signals of BDS-3 test satellites, B1C signal has the worst pseudorange measurement accuracy while B2a+b signal has the best; the pseudorange measurement accuracy of Bs signal is worse than that of B2a+b signal, but better than that of B1C signal.

(2) The multipath effects of the pseudorange measurements of BDS-3 are less than that of BDS-2, and there is no obvious systematic errors associated with satellite elevation exist in the pseudorange measurements of BDS-3. Among the different signals of BDS-3, B2a+b signal has the strongest anti-multipath ability, while the B1C has the worst.

(3) In the aspects of signal-in-space quality and the timing accuracy, the UERE values indicate that the user equivalent range error of MEO satellites is better than that of IGSO satellites; and the overall UERE is smaller than 0.73 m. The timing accuracy is usually better than 10 ns and the worst accuracy is about 21.9 ns.

(4) According to the simulation analysis of BDS-3 constellation, the number of visible satellites of BDS-3 in global scale is about 6 to 13, the global PDOP value is between 1.3 and 2.7, the HDOP value is between 0.7 and 1.5, and the VDOP value is between 1.1 and 2.4. When the UERE is 1 m, the global positioning accuracy is expected to achieve 1.3–2.7 m, the horizontal positioning accuracy is estimated at 0.7–1.5 m, and the elevation positioning accuracy is estimated at 1.1–2.4 m.

It should be pointed out that the performance of BDS-3 system will be further verified and analyzed with the long-term operation and observation of the BDS-3 demonstration system satellites and the launch of BDS-3 network satellites. Other performance, such as integrity (Xu et al., 2013; Yang and Xu, 2016), reliability and robustness should also be studied.

Acknowledgements *This work was supported by National Key R&D Program of China (Grant Nos. 2016YFB0501700, 2016YFB0501701) and National Natural Science Foundation of China (Grant No. 41374019).*

References

Chen J P, Hu X G, Tang C P, Zhou S S, Guo R, Pan J Y, Li R, Zhu L F. 2016. Orbit determination and time synchronization for new-generation Beidou satellites: Preliminary results (in Chinese). Sci Sin-Phys Mech Astron, 46: 119502

China Satellite Navigation Office. 2013. BeiDou Navigation Satellite System Open Service Performance Standard (Version 1.0)

China Satellite Navigation Office. 2017a. BeiDou Navigation Satellite System Signal in Space Interface Control Document Open Service Signal B1C and B2a (Test Version)

China Satellite Navigation Office. 2017b. Update on BeiDou Navigation Satellite System, ICG-12, 3 December 2017, Kyoto, Japan

de Bakker P F, van der Marel H, Tiberius C C J M. 2009. Geometry-free undifferenced, single and double differenced analysis of single frequency GPS, EGNOS and GIOVE-A/B measurements. GPS Solut, 13: 305–314

Feng Y. 2008. GNSS three carrier ambiguity resolution using ionosphere-reduced virtual signals. J Geod, 82: 847–862

Geng J, Bock Y. 2014. Erratum to: Triple-frequency GPS precise point positioning with rapid ambiguity resolution. J Geod, 88: 95–97

Gu J X, Wang C F, Song Z G. 2015. Channel performance testing and analysis of BeiDou short-message communication (in Chinese). Meteorol Sci Technol, 43: 458–463

Guo F, Li X, Zhang X, Wang J. 2016. Assessment of precise orbit and clock products for Galileo, BeiDou, and QZSS from IGS Multi-GNSS Experiment (MGEX). GPS Solut, 21: 279–290

Han C H, Cai Z W, Lin Y T, Xiao S H, Zhu L F, Wang X L. 2013. Time synchronization and performance of BeiDou satellite clocks in orbit. Int J Navig Observat, doi: 10.1155/2013/371450

Han C, Yang Y, Cai Z. 2011. BeiDou Navigation Satellite System and its time scales. Metrologia, 48: S213–S218

He H, Li J, Yang Y, Xu J, Guo H, Wang A. 2014. Performance assessment of single- and dual-frequency BeiDou/GPS single-epoch kinematic positioning. GPS Solut, 18: 393–403

He L, Ge M, Wang J, Wickert J, Schuh H. 2013. Experimental study on the precise orbit determination of the BeiDou Navigation Satellite System. Sensors, 13: 2911–2928

Li B F, Shen Y, Zhang X. 2013. Three frequency GNSS navigation prospect demonstrated with semi-simulated data. Adv Space Res, 51: 1175–1185

Li B F, Li Z, Zhang Z T, Tan Y A. 2017. ERTK: Extra-wide-lane RTK of triple-frequency GNSS signals. J Geod, 1031–1047

Li J L, Yang Y X, He H B, Xu J Y, Guo H R. 2012. Optimal carrier-phase combinations for triple frequency GNSS derived from an analytical method. Acta Geodetica et Cartographica Sinica, 41: 797–803

Li J L, Yang Y X, Xu J Y, He H B, Guo H R. 2013. GNSS multi-carrier fast partial ambiguity resolution strategy tested with real BDS/GPS dual- and triple-frequency observations. GPS Solut, 19: 5–13

Li J L, Yang Y X, He H B, Guo H R. 2017. An analytical study on the carrier-phase linear combinations for triple-frequency GNSS. J Geod, 91: 151–166

Montenbruck O, Steigenberger P, Hauschild A. 2015. Broadcast versus precise ephemerides: a multi-GNSS perspective. GPS Solut, 19: 321–333

Peng H, Yang Y, Wang G, He H B. 2016. Performance Analysis of BDS Satellite Orbits during Eclipse Periods: Results of Satellite Laser Ranging Validation (in Chinese). Acta Geodaet Cartograph Sin, 45: 639–645

Ren X, Yang Y, Zhu J, Xu T. 2017. Orbit determination of the Next-Generation Beidou satellites with Intersatellite link measurements and a priori orbit constraints. Adv Space Res, 60: 2155–2165

Shi C, Zhao Q, Hu Z, Liu J. 2013. Precise relative positioning using real tracking data from COMPASS GEO and IGSO satellites. GPS Solut, 17: 103–119

Shi C, Zhao Q L, Li M, Tang W M, Hu Z G, Lou Y D, Zhang H P, Niu X J, Liu J N. 2012. Precise orbit determination of Beidou Satellites with precise positioning. Sci China Earth Sci, 55: 1079–1086

Tan S S. 2010. The Engineering of Satellite Navigation and Positioning. 2nd ed. Beijing: National Defense Industry Press

Tan S S. 2017. Innovation development and forecast of BeiDou system (in Chinese). Acta Geodaet Cartograph Sin, 46: 1284–1289

Tang C P, Hu X G, Zhou S S, Pan J Y, Guo R, Hu G M, Zhu L F, Li X J, Wu S, Wang Y. 2017. Centralized autonomous orbit determination of Beidou navigation satellites with inter-satellite link measurements: preliminary results (in Chinese). SSPMA, 47: 029501

Wanninger L, Beer S. 2015. BeiDou satellite-induced code pseudorange variations: diagnosis and therapy. GPS Solut, 19: 639–648

Xu J Y, Yang Y X, Li J L, He H B, Guo H R. 2013. Integrity analysis of COMPASS and other GNSS combined navigation. Sci China Earth Sci,

56: 1616–1622
Yang Y X. 2010. Progress, contribution and challenges of Beidou satellite navigation system. Acta Geodaet Cartograph Sin, 39: 1-6
Yang Y X, Li J L, Xu J Y, Tang J, Guo H R, He H B. 2011. Contribution of the Compass satellite navigation system to global PNT users. Chin Sci Bull, 56: 2813–2819
Yang Y X, Li J L, Wang A B, Xu J Y, He H B, Guo H R, Shen J F, Dai X. 2014. Preliminary assessment of the navigation and positioning performance of BeiDou regional navigation satellite system. Sci China Earth Sci, 57: 144–152
Zhang X H, Ding L L. 2013. Quality Analysis of the second generation Compass observables and stochastic model refining. Geomatics Inform Sci Wuhan Univ, 38: 832–836
Yang Y, Xu J. 2016. GNSS receiver autonomous integrity monitoring (RAIM) algorithm based on robust estimation. Geodesy Geo Dyn, 7: 117–123

(Responsible editor: Dinghui YANG)